Title
Creep in Shear of Experimental Solder Joints

Authors
Tribula, D.B.
Morris, J.W.

Publication Date
1989-09-01

Center for Advanced Materials

CAM

To be presented at the ASME Winter Annual Conference,
San Francisco, CA, December 10–14, 1989, and
to be published in the Proceedings

Creep in Shear of Experimental Solder Joints

D. Tribula and J.W. Morris, Jr.

September 1989

Materials and Chemical Sciences Division

Lawrence Berkeley Laboratory • University of California

ONE CYCLOTRON ROAD, BERKELEY, CA 94720 • (415) 486-4755

Prepared for the U.S. Department of Energy under Contract DE-AC03-76SF00098

DISCLAIMER

LBL 27775

Creep in Shear of Experimental Solder Joints

D. Tribula and J. W. Morris, Jr.

Center for Advanced Materials
Materials and Chemical Sciences Division
Lawrence Berkeley Laboratory
1 Cyclotron Road
Berkeley, CA 94720
and
Department of Materials Science and Mineral Engineering
University of California

September 1989

This work is supported by the Director, Office of Energy Research, Office of Basic Energy Science, Materials Sciences Division of the U. S. Department of Energy under Contract No. *DE-AC03-76SF00098*

Creep in Shear of Experimental Solder Joints

D. Tribula and J.W. Morris, Jr.

Center for Advanced Materials, Lawrence Berkeley and
Department of Materials Science
University of California at Berkeley

Thermal fatigue failures of solder joints in electronic devices are a great concern in the electronics industry. Since the fatigue load is often in shear the details of thermal fatigue failure in shear are of particular interest. Recent work indicates that similar failure mechanisms operate in both thermal fatigue in shear and unidirectional creep in shear. Additionally, since the operative temperatures during thermal fatigue represent high solder homologous temperatures, creep deformation is certainly involved. These factors and the relative ease of conducting creep experiments encourage the study of solder joints under shear creep conditions. This work presents steady state shear creep rate vs. shear stress data for several solder compositions, including the binary eutectic alloy and Pb-Sn alloyed with small amounts of Bi, Cd, In, and Sb, in a joint configuration. These data indicate that conventional creep mechanisms operate in the temperature and shear strain rate ranges studied. Extensive microstructural information is also reported. The microstructural evolution under creep conditions indicates that the instability of the as-cast binary Pb-Sn eutectic microstructure initiates creep failure. Changes of the as-solidified microstructure with the third element addition are reported as are the microstructural responses of each of these alloys to creep deformation. The efficacy of postponing the microstructural instability with the addition of small amounts of ternary elements is discussed.

INTRODUCTION

Pb-Sn solders are a critical component of most electronic devices. A solder joint provides both the vital mechanical and electrical connection between and within the many levels of an electronic package. Increased device miniaturization and the desire for faster circuit operation necessitate a very high degree of reliability of all solder contacts. However, this particular application constitutes rather severe operating conditions for the solder, and the contact is liable to failure, specifically failure by thermal fatigue of the solder joints.

The solder contact most often joins materials of dissimilar thermal expansion characteristics, e.g. a ceramic chip carrier and a polymeric circuit board. Service conditions entail temperature changes, especially cyclic temperature changes: Joule heating and cooling associated with a simple on/off cycle, and environmental temperature changes such as those experienced by aircraft and automobile components. Every high temperature excursion results in a straining of the solder joint as the constraining materials expand different amounts. A cooling period reverses the strain experienced by the joint and

essentially concludes a fatigue cycle. The details of the deformation extent and state vary with the operating conditions and specific joint geometry. However, the deformation is most often in shear, and, as a consequence of the low melting point of the solder, occurs at relatively high solder homologous temperatures. In fact, the loading conditions that result from the temperatures changes constitute low strain rate low-cycle fatigue of the solder joint.

Increased solder joint reliability requires the development of an accurate life prediction model that will allow a solder joint to be removed from service prior to failure. Alternately, an understanding of the mechanisms that cause fatigue failures will indicate appropriate metallurgical changes to defeat these mechanisms and thus yield an improved, more fatigue resistant solder alloy.

An understanding of the creep behaviour of a solder joint addresses both these issues. An accurate life prediction model must reproduce and account for all the operating conditions experienced by the solder joint in service on an accelerated laboratory time scale. The elevated service temperatures and operative strain rates imply that creep is a major deformation mode during the fatigue cycle. An accurate representation of the creep response of a solder joint is thus needed as part of an accurate life prediction model. Secondly, the observation that solder joint fatigue failures and creep failures appear the result of similar metallurgical mechanisms indicates that both techniques can be used to study and evaluate the fatigue failure mechanism and relative solder alloy fatigue resistance.

The scope of this work is twofold. Firstly, the creep behaviour of several solder alloys is studied to determine a constitutive equation to represent the high temperature time dependent deformation of a solder joint. Secondly, as part of an on-going effort to identify the solder fatigue mechanism, this work will determine the microstructural response of a solder joint whose microstructure has been changed via a third element addition.

A series of creep experiments was conducted on each of six alloys: two binary compositions, eutectic and 60Sn-40Pb and a 58Sn-40Pb-2X series where X was Bi, Cd, In and Sb. Creep data were collected and analyzed in terms of a power law dependence between strain rate and stress and the appropriate constants were determined. Additionally, microstructural observations were made as a function of the creep deformation. Initial, as-deformed, and deformed polished joints were examined and evaluated.

EXPERIMENTAL

A schematic illustration of the sample used in this work appears in Figure 1. The sample is a three layer Cu sandwich joined with solder. The hole and slot configuration has the consequence that on tensile loading the enclosed solder joint regions (shaded areas in figure) are deformed in nearly simple shear. Sample preparation consisted of a polish and etch of the Cu plates, assembly with appropriate spacers to yield the desired joint width, and immersion into a molten solder bath. A final machining step yielded the specimen shown in the Figure. Each joint was examined both prior to deformation and

immediately after. The surface relief that is associated with deformation was clearly visible under an optical microscope. A final polish and etch of the deformed joint was performed, and the initial, as-deformed and final microstructures were compared.

Creep loading was done in an oil bath whose temperature was maintained to ±2°C. Temperatures ranged from 20°C to 125°C. An extensometer was positioned such that it straddled the shaded areas of the solder joint. Joint extension was continuously monitored on a chart recorder. Shear strain was calculated as joint elongation divided by the initial joint width, .020" (0.5 mm).

RESULTS

Creep Data

Figure 2 shows a typical creep curve. All three creep regimes are exhibited. Primary creep is active for the first ~2% of the creep strain. This was true for all specimens tested. Primary creep is short-lived; however, it was present in all specimens tested. The steady state regime consumes the next ~10% strain. All samples exhibited an obvious second stage creep regime, although its extent varied from sample to sample. No correlation between the extent of steady state creep and the solder composition was apparent. In all cases, the tertiary range consumed at least one half of the creep life.

A plot of the strain rate in the steady state creep range, at constant temperature, vs. the corresponding stress allows for the determination of the stress exponent, n. A typical plot is shown in Figure 3. The linearity of the data on the log/log plot indicate a power law dependence between strain rate and stress. In this particular case, the slope, the stress exponent, has a value of 6.0.

A plot of the steady state strain rates, at a constant stress, vs. inverse temperature allows for the determination of the activation energy, E_a. A typical plot is shown in Figure 4. Linearity on the semilogarithmic plot is characteristic of an Arrhenius type temperature dependence. The data for the Cd alloy shown here indicate an activation energy for creep of 16 kcal/mole.

All the data are listed in Table 1. The A', n, and E_a values refer to the folowing equations:

$$\frac{d\gamma}{dt} = A' \tau^n \; ; \; A' = A \, e^{-E_a/kT} .$$

The values of n were obtained at 75°C and the activation energies at 1280 psi.

Table 1.

	A'	n	E_a (kcal/mole)
60Sn-40Pb	3×10^{-25}	6.3	20
61.9Sn-38.1Pb	4×10^{-24}	6.0	19
58Sn-40Pb-2Bi	5×10^{-22}	5.5	17
58Sn-40Pb-2Sb	3×10^{-22}	5.6	16
58Sn-40Pb-2Cd	1×10^{-18}	3.7	16
58Sn-40Pb-2In	9×10^{-17}	3.8	*

Microstructures

The solder microstructures are also of great importance. The initial 60Sn-40Pb microstructure appears in Figure 5. The microstructure is a mixture of the Pb-rich and Sn-rich phases. (Pb-rich phase appears dark and the Sn-rich phase appears light in optical microscopy). The Pb-rich phase appears both as primary Pb-rich dendrites and as a constituent of the eutectic microstructure. The eutectic microstructure consists of alternating Pb-rich and Sn-rich phase regions distributed within eutectic colonies. A specific phase particle size and shape arrangement distinguishes a single eutectic colony. In this sense, the colony macrostructure contains the eutectic microstructure. The phase particle morphology within a colony may be lamellar or globular. The boundary between neighboring colonies is often very distinct and delimited by a narrow region of enlarged equiaxed phase particles.

The as-solidified microstructures of the ternary alloys are shown in Figures 6 and 7. All specimens were manufactured using identical processing techniques, hence microstructural changes are a result of compositional changes only. The addition of Sb has little influence on the microstructure. A microstructure exhibiting distinct individual eutectic colonies exists. Phase particle sizes and shapes are similar to those observed for the 60-40 alloy. This contrasts with the microstructure of the Bi alloyed solder. The Bi addition changes the character of both the colony macrostructure and the eutectic microstructure within. The colony structure appears equiaxed and smaller relative to the binary and Sb alloys. The eutectic structure within the colonies is no longer uniform, but varies from the colony center to the colony periphery. The central zone consists of fine, parallel phase particles. The peripheral zone is composed of enlarged phase particles of smaller aspect ratio. A similar microstructure is observed for the In alloyed solder: small colonies consisting of both fine and coarse phase particles. Compared to the Bi-alloyed solder, the colonies are smaller and the boundary area between colonies is not as wide and distinct. The Cd-alloyed solder exhibits the least distinct colony structure. Small regions of fine parallel phase particles are observed, however they comprise a smaller fraction of the sample than that taken up by the inter-colony microstructure. In contrast to the alloys

previously discussed, the intra-colony microstructure is equiaxed with no apparent regular arrangement between the two phases.

To summarize, the addition of the third element appears to affect the colony macrostructure and as well as the eutectic microstructure contained therein. All ternary alloys exhibited a refinement of the eutectic colony size relative to the binary alloy. Also very distinct is the appearance of diffuse colony boundaries with the addition. The greatest colony size refinement is observed with the In-alloyed solder. The boundary area width (on a two-dimensional metallographical section) increases most significantly with the Bi and Cd additions. It is also interesting that the average phase particle diameter of the Bi, Cd and In alloys is far coarser than that of either the Sb or simple binary alloy.

Figure 8 shows the microstructure that evolves within a 63Sn-37Pb solder joint as it is crept. A band of equiaxed microstructure has developed along the length of the joint parallel to the copper/solder interface. In Figure 9 the same joint appears at a slightly lower magnification. This band of coarser microstructure runs along the entire length of the joint is is quite distinct from the remaining "background" eutectic microstructure. Within this band, the grain size and shape of both phases are similar, uniform, and equiaxed. No trace of the initial as-solidified eutectic colony structure remains. Figure 9 (left) shows that the deformation is highly localized to a narrow band parallel to the Cu-solder interface. Secondary deformation occurs at irregular intervals roughly perpendicular to this major deformation band. A comparison of this microstructure with the surface relief that develops across the joint as it is deformed reveals that the areas of maximum surface relief correspond exactly with the location of this coarsened microstructure, Figure 9 left and right.

In Figures 10 and 11 the same comparison is made for the Bi and Sb alloys. In both cases the deformation patterns observed are highly nonuniform; most deformation has taken place in a narrow band parallel to the copper-solder interface. Comparing the deformation patterns (Figure 10) with the corresponding polished microstructures (Figure 11), it is obvious that a "new" microstructure has evolved at the site of maximum deformation. The new microstructure is uniform and equiaxed and does not resemble the initial as-solidified eutectic colony structure present prior to deformation.

The microstructure and deformation patterns of the Cd and In alloyed solders are shown in Figures 12 and 13. No single plane of maximum deformation is apparent. The deformation patterns are uniform across the entire width of the solder joint. This is true for both Cd and In solders. Examination of the associated microstructures reveals no significant microstructural changes. Samples that were crept at high temperatures exhibited some homogeneous coarsening of the as-solidified microstructure, however, no local microstructural changes such as those observed with the other alloys were found.

DISCUSSION

Creep Data

The high temperature steady state deformation of many alloy systems can be represented by the following equation :

$$\frac{d\gamma}{dt} = A\tau^n e^{-E_a/kT},$$

where $d\gamma/dt$ is the steady-state shear strain rate and τ is the shear stress. The value of the stress exponent, n, and activation energy, E_a, within a given strain rate/stress regime is characteristic of the operative deformation mechanism. For example, conventional dislocation climb controlled steady state creep is characterized by a stress exponent in the range of 4~7 and an apparent activation energy on the order of that for self diffusion (e.g. Bird et al., 1964, and Weertman and Weertman, 1983). Bulk eutectic Pb-Sn samples are known to behave according to this equation. Specifically, deformation in the conventional climb-controlled creep regime is characterized by a stress exponent of 6~7 and an activation energy equal to ~20 kcal/mole (Zehr and Backhofen, 1968; Grivas et al., 1979; Rohde and Swearengen, 1980; Kashyap and Murty, 1982; Weinbell et al., 1987).

However, it should be made clear that different deformation mechanisms, and hence different n and E_a values, are possible with different microstructures within this single alloy system. For example, a worked and annealed, i.e. a recrystallized Pb-Sn microstructure, in addition to possessing a dramatically different microstructure also exhibits dramatically different deformation characteristics. The recrystallized microstructure consists of a uniform distribution of equiaxed grains of both the Pb-rich and Sn-rich phases, and bears little resemblance to the parent as-solidified morphology, such as that studied here (e.g., Avery and Backhofen, 1965; Cline and Alden, 1967; Grivas, 1974). This recrystallized Pb-Sn is known to go through several deformation regimes, each subject to different rate controlling mechanisms and each with a characteristic value of the stress exponent and activation energy. Within the strain rate/stress/temperature regime studied in this work, a recrystallized Pb-Sn microstructure is expected to behave superplastically with a characteristic stress exponent ~2 and an activation energy equal to that of grain boundary diffusion, 12 kcal/mole (Bird et al., 1964; Zehr and Backhofen, 1968; Mohamed and Langdon, 1975; Grivas et al., 1978 and 1979; Kashyap and Murty, 1981 and 1982). Additionally, superplastic creep occurs without a primary creep regime. Deformation, following an initial transient, immediately occurs at a constant strain rate (e.g., Bird et al., 1964, and Grivas, 1974).

The current work is done on as-solidified microstructures, microstructures that are not expected to deform superplastically. The values of the constants n and E_a found in this work are consistent with this expectation and are representative of conventional creep mechanisms. Furthermore, all specimens exhibited a finite primary creep range, a phenomenon again consistent with the above mentioned mechanism.

In addition to data for bulk Pb-Sn deformation, there is some limited data available on the creep deformation characteristics of solder joints. The values of the stress exponents reported for solder joints range from ~2-6 (Solomon, 1986; Hall, 1987; Enke and Sandor, 1988; Shine and Fox, 1988). The different joint geometries and joint processing techniques used in each of these experiments may account for the scatter in the reported n values. No similar data is available for the ternary alloys. However, the data as shown in Table 1 indicate no significant changes in either the stress exponent nor activation energy with third element addition.

It is, however, very interesting that the stress exponents for the Cd and In alloys are consistently lower than the others. Recall that these two alloys also exhibited the unique microstructural behaviour. In both cases the lower stress exponent is also associated with uniform deformation and no apparent local microstructural instability with deformation; the coarsened bands that are known to initiate joint failure do not form in these two alloys.

Microstructures

Near eutectic Pb-Sn solder joint failures have long been associated with a coarsening of the as-solidified solder microstructure at the failure site (Wild, 1975; Bangs and Beal, (1978); Wolverton, 1987; Frear et al., 1988a and b; Tribula et al., 1989a and b). The mechanism that leads to the formation of such coarsened microstructural regions has recently been proposed (Tribula et al., 1989b). The development of an inhomogeneous shear deformation pattern within the solder microstructure results in regions of concentrated shear within the solder joint. These trigger a recrystallization of the as-solidified microstructure to relieve the accumulated deformation within the shear band. Subsequent grain growth results in the observed coarsened and equiaxed microstructure. Both the tendency toward nonuniform shear deformation and microstructural instability under high temperature deformation are inherent to the as-solidified Pb-Sn solder and contribute to the failure of the Pb-Sn joint. A solder microstructure that deforms uniformly and resists recrystallization should thus defeat these failure mechanisms and so exhibit improved fatigue resistance.

Changes to the as-solidified microstructure are expected through additions of a third element to the binary alloy. Small additions to the binary alloys may be treated analogously to the case of an impurity in a single phase alloy. As solidification proceeds , the rejection of the impurity into the liquid results in a region of supercooled liquid and thus a breakdown of solidification front, i.e. the cellular/colony structure. Coarser phase particles result from the slower growth rate caused by the time needed for the accumulating impurity to diffuse away from the solidification front so that further solidification may take place (Weart and Mack, 1958; Kraft, 1966; Quan, 1988).

The actual solidification conditions in the solder joint are not known. However, the colony size refinement may be rationalized through the supercooling effect that results with the third element addition. The diffuse and coarse boundary structure may be due to the slower growth rate associated with increasing concentration of the third element ahead of the solid/liquid interface.

The as-solidified morphology is critical in determining deformation paths. The surface relief exhibited after deformation of an equiaxed (recrystallized) microstructure appears uniform throughout the entire sample. Relief occurs within individual phase grains as well as at intra- and inter- phase boundaries. This contrasts with the surface relief observed for a deformed as-solidified microstructure. The surface relief is localized to the colony boundaries. The fine regular arrangement of phase particles within the colony moves as one piece. Recall that the colony boundary area consists of phase particles that appear the most equiaxed and occur with the least evidence of a specific phase to phase arrangement. In this sense, the boundary area morphologically resembles the recrystallized microstructure. It is well known that a recrystallized, equiaxed Pb-Sn microstructure is much softer than the as-solidified one (e.g. Cline and Alden, 1967). It thus seems likely that the softest material within the as-solidified microstructure is that in the colony boundary area and thus will deform first.

The addition of the third element may refine the colony size and/or increase the colony boundary area. Both events result in a larger fraction of "soft", easily deformable solder microstructure. Joint deformation is thus accommodated over a larger area and the stress intensities needed to initiate a recrystallization are not realized. Hence, the microstructure does not change with deformation. The Cd alloyed microstructure possesses the smallest area of fine regularly arranged phase particles and the greatest area of apparently equiaxed phase particles; this alloy also exhibits uniform surface relief and microstructural stability with deformation. The In-alloyed solder has a small colony size and thus a large fraction of equiaxed boundary area. Again the deformation is uniform and no local microstructural changes are observed. The Bi solder does show a diffuse colony boundary area, however the arrangement of phase particles within a colony is not random. The phase particles, though coarsened, are regularly arranged as alternating lamellae of the two phases. The deformation in this solder is nonuniform. The Sb alloyed solder also deforms nonuniformly. The colony size is small containing a highly regular arrangement of Pb and Sn rich lamellae, and the boundary area is very narrow. Both the Bi and Sb alloyed solders are liable to the recrystallization phenomenon observed in the 60/40 alloy.

Solder joint fatigue failures - actual service failures as well as failures observed in the laboratory on experimental solder joints - are associated with a coarsening of the solder microstructure at the eventual failure site (Bangs and Beal, 1978; Wild, 1975; Wolverton, 1987; Frear et al., 1988a and b; Tribula et al., 1989a and b). This same phenomenon is observed under creep deformation conditions and is directly related to the highly localized deformation that develops as the joint is strained. The localized deformation is in turn a consequence of the inhomogeneity of the as-solidified microstructure. The addition of a third element to the binary Sn-Pb solder changes the as-solidified microstructure and thus the observed deformation patterns. The addition of a small amount of Cd or In results in a microstructure that exhibits much more uniform deformation behaviour, and joint failures are not associated with a local microstructural changes.

Regarding the design of solders with improved fatigue resistance, the current results suggest that the Cd and In alloyed solders show great promise since these alloys posses microstructures that suppress the formation of the local coarsening that governs

solder joint failures. In fact, preliminary results on the thermal fatigue resistance of these solders indicate improved thermal fatigue resistance with the Cd and In addition. This work is currently in progress.

CONCLUSIONS

The creep behaviour of solder joints in the strain rate regime 10^{-3} to 10^{-6} sec^{-1} appears to be a conventional climb controlled mechanism. Both the value of the determined stress exponent, 6, and activation energy, 20 kcal/mole, are consistent with this mechanism. The addition of small amounts (2 wt%) of a third element, Bi, Cd, In, Sb does not dramatically alter these values. A dramatic difference is, however, observed in the microstructural response to creep deformation. The In and Cd alloys both exhibited uniform deformation under creep conditions and possessed microstructures that were stable under creep deformation conditions. This is in great contrast with the behaviour observed with the Bi, Sb, and both binary alloys. These four deformed in a highly localized manner, and the localized deformation was associated with the evolution of a coarsened equiaxed microstructure wherein the joint failure eventually occurred. It is interesting that this difference in microstructural response to deformation is consistent with the slightly lower stress exponents determined for the In- and Cd-alloyed solders.

The microstructural response of each alloy may be rationalized in terms of the morphology of the as-solidified microstructure. Those microstructures that posses the greatest areas of regular, seemingly ordered phase arrangements, the binary, Bi and Sb solders, are liable to inhomogeneous deformation. Microstructures composed of large areas of more equiaxed irregular phase particle arrangements tend to deform more uniformly. The microstructures that deform uniformly are desirable since they remain stable under high temperature shear deformation and thus defeat the formation of a locally coarsened solder microstructure that is associated with joint failure. Since this same mechanism is operative under thermal fatigue conditions, the results of this work indicate that the Cd and In alloys warrant further study under more representative operating conditions.

ACKNOWLEDGEMENT

This work was supported by the Director, Office of Energy Research, Office of Basic Energy Science, Materials Science Division of the U.S. Department of Energy, under contract No. DE-AC03-76SF00098.

REFERENCES

D. H. Avery and W.A. Backhofen, (1965), Trans. ASM, 58 pp. 551-562.

E.R. Bangs, R.E. Beal, (1978), Weld. Res. Supp., Weld. J., 54 pp. 377-383.

J.E. Bird, A.K. Mukherjee, J.F. Dorn, (1964), Quantitative Relation Between Properties and Microstructure, Israel University Press, pp. 255-342.

H.E. Cline and T.H. Alden, (1967), Trans. Met. Soc. AIME, 239 pp. 710-714.

N.F. Enke and B.I. Sandor, (1988), ASME publication 88-WA/EEP-12, .

D.Frear, D. Grivas, J.W. Morris, Jr., (1988a), J. Elect. Mat., 17 pp. 171-180.

D.R. Frear, D. Grivas, J.W. Morris, Jr., (1988b), J. Met., 40 pp. 19-22.

D. Grivas, (1974), "Steady State Creep in Pb-Sn Eutectic Alloys", M.S. thesis, University of California, Berkeley.

D. Grivas, (1978), "Deformation of Superplastic Alloys at relatively Low Strain Rates", Ph.D. thesis, University of California, Berkeley.

D. Grivas, K.L. Murty, and J.W. Morris, Jr., (1979), Acta. Met., 27 pp. 731-737.

P.M. Hall, (1987), EEE Trans., CHMT-12 pp. 556-565.

B.P. Kashyap, G.S. Murty, (1981), Mat. Sci. and Eng., 50 pp. 205-213.

B.P. Kashyap, G.S. Murty, (1982), Met. Trans. A, 13A pp.53-58.

R.W. Kraft, (1966), J. Met., 2 pp. 192-200.

F.A. Mohamed and T.G. Langdon, (1975), Phil. Mag., 32 pp. 697-709.

L.K. Quan, (1988), "Tensile and Shear Behaviour of Alloyed Sn-Pb Solder Joints", M.S. thesis, University of California, Berkeley.

R.W. Rohde and J.C. Swearengen, (1980), Trans. ASME, J. Eng. Mat. and Tech., 102 pp. 207-214.

M.C. Shine and L.R. Fox, (1988), Low Cycle Fatigue, ASTM STP 942, H.D. Solomon, Ed., American Society for Testing and Materials, Philadelphia, pp. 588-610.

H.D. Solomon, (1986), Braz. and Sold., 11 pp.68-75.

D. Tribula, D. Grivas, D.R. Frear, and J.W. Morris, Jr., (1989a), Trans. ASM, J. Elect. Pack., pp.83-.

D. Tribula, D. Grivas, D.R. Frear, and J.W. Morris, Jr., (1989b), to be published, Weld. Res. Sup. Weld. J., October 1989.

H.W. Weart and D.J. Mack, (1958), Trans. Met. Soc. AIME, 10 pp. 664-670.

J. Weertman and J.R. Weertman, (1983), Physical Metallurgy, R.W. Cahn, P. Haasen, Eds., Elsevier Science Publishers, pp. 1310-1340.

R.C. Weinbell, J.K. Tien, R.A. Pollack, and S.K. Kang, (1987), J. Mat. Sci., pp. 3901-3906.

R.N. Wild, (1975), "Some Fatigue Properties of Solder and Solder Joints", IBM Report no. 74z000481, October, 1975.

W.M. Wolverton, (1987), Braz. and Sold., 13 pp. 33-45.

S.W. Zehr , W.A. Backhofen, (1968), Trans ASM, 61 pp. 300-373.

FIGURE CAPTIONS

Figure 1. The specimen configuration used in the creep test. The shaded areas are the solder joints of interest. On tensile loading these areas are loaded in simple shear. Planes of maximum shear run parallel to the Cu/solder interface. The micrographs shown in this paper each represent a portion of one of these shaded areas. In all cases, the micrograph orientation is such the loading/shear direction runs horizontally across the image.

Figure 2. A creep curve for the 58Sn-40Pb-2Sb alloy. Extensive secondary and tertiary creep regions are apparent as is a small primary creep stage. Such a curve was typical of all the samples studied.

Figure 3. A plot of strain rate vs. stress, at constant temperature for the 61.9Sn-38.1Pb alloy. The slope of the line is equal to 6.0.

Figure 4. A plot of steady state strain rate vs. inverse temperature at a constant stress for the 58Sn-40Pb-2Cd alloy. The slope of the line indicates an activation energy for steady state creep of 16 kcal/mole.

Figure 5. The initial 60Sn-40Pb joint microstructure. Lead rich areas are dark, Sn-rich areas are light.

Figure 6. The initial microstructures of the ternary alloys studied: (top) 58Sn-40Pb-2Sb, (bottom) 58Sn-40Pb-2Bi.

Figure 7. The initial microstructures of the ternary alloys studied: (top) 58Sn-40Pb-2In, (bottom) 58Sn-40Pb-2Cd.

Figure 8. A high magnification micrograph showing the microstructural detail within a coarsened band. The grain morphology within this band is uniform and equiaxed. No colony-like features are apparent.

Figure 9. A 61.9Sn-38.1Pb solder joint. (top) The surface relief that develops within the bulk of the joint under creep deformation. (bottom) The same surface after a light polish. There exists an exact correspondence between the location of the coarsened microstructure and the location of maximum surface deformation.

Figure 10. The surface relief observed after creep deformation of the (a) Sb- and (b) Bi-alloyed solders. The deformation patterns reveal highly localized deformation occurring adjacent and parallel to the copper-solder interface.

Figure 11. The polished microstructures of the crept (a) Sb- and (b) Bi-alloyed solder joints. A band of coarsened microstructure similar to that observed in the simple binary alloys is visible. The location of the coarsened band corresponds with the site of maximum deformation.

Figure 12. The surface relief observed after creep deformation of the (a) Cd- and (b) In-alloyed solders. The deformation patterns reveal uniform deformation occurring throughout the entirety of the joint.

Figure 13. The polished microstructures of the crept (a) Cd- and (b) In-alloyed solder joints. The microstructures are similar to those prior to deformation.

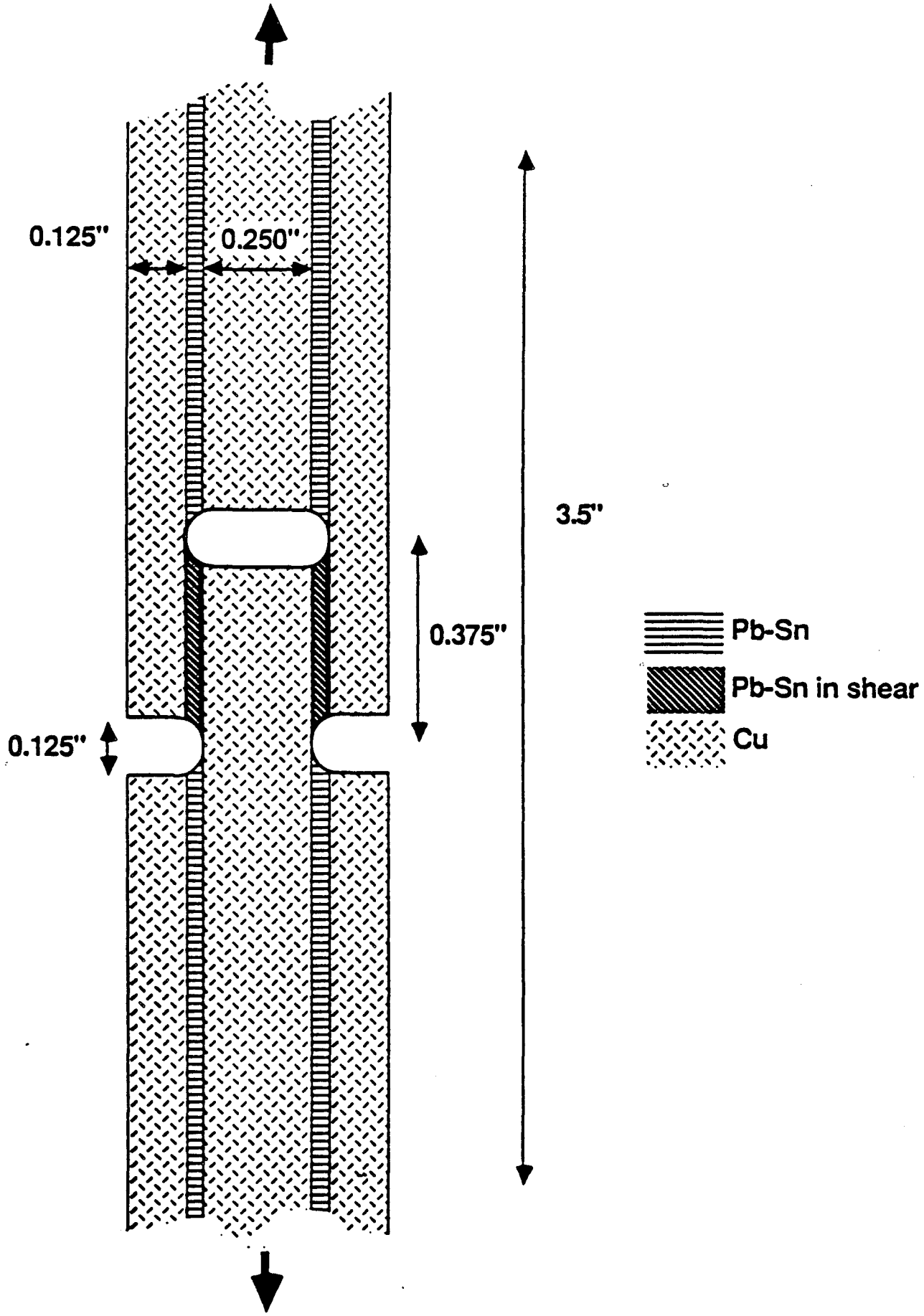

Figure 1

STRAIN vs TIME

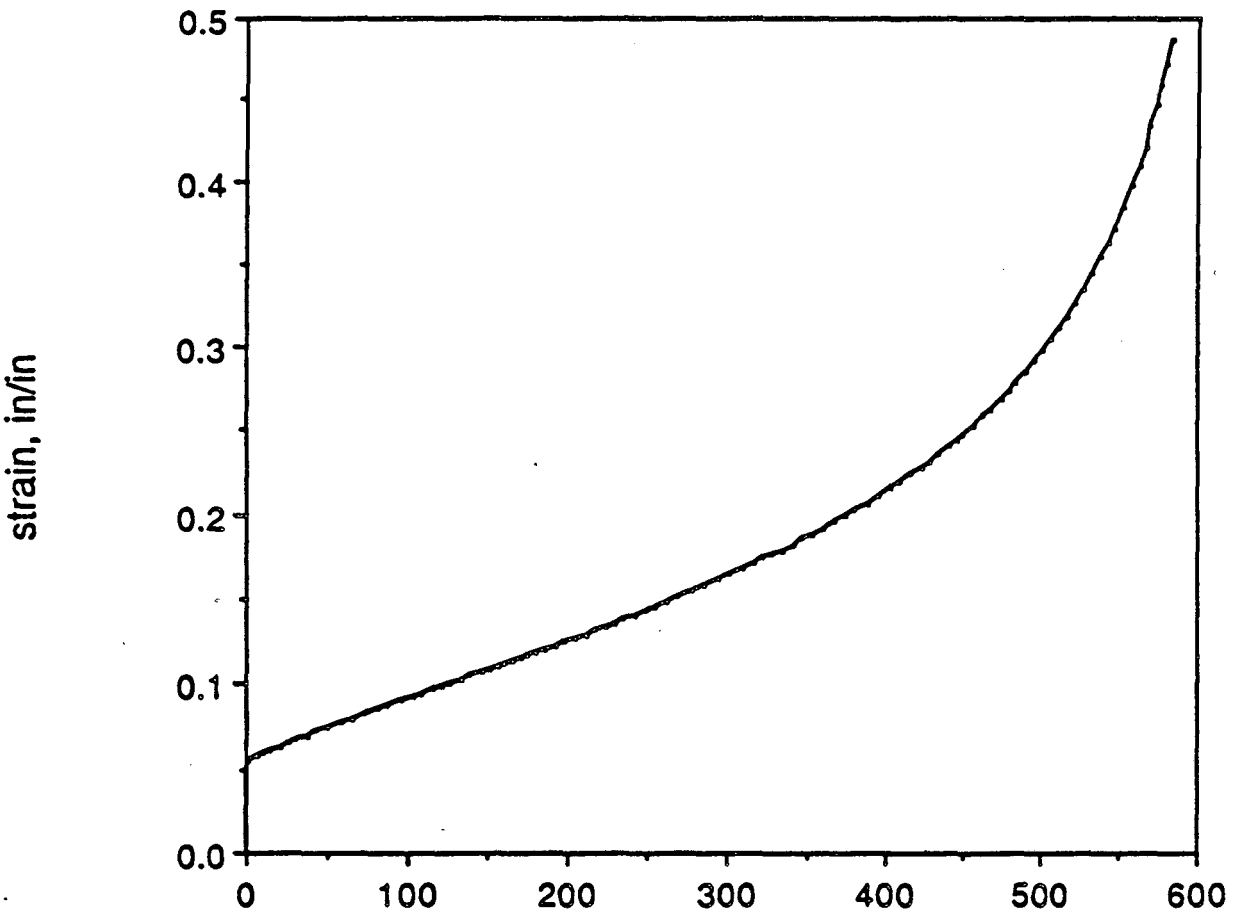

58Sn-40Pb-2Sb, 125 C 1280 psi

Figure 2

STRAIN RATE vs STRESS

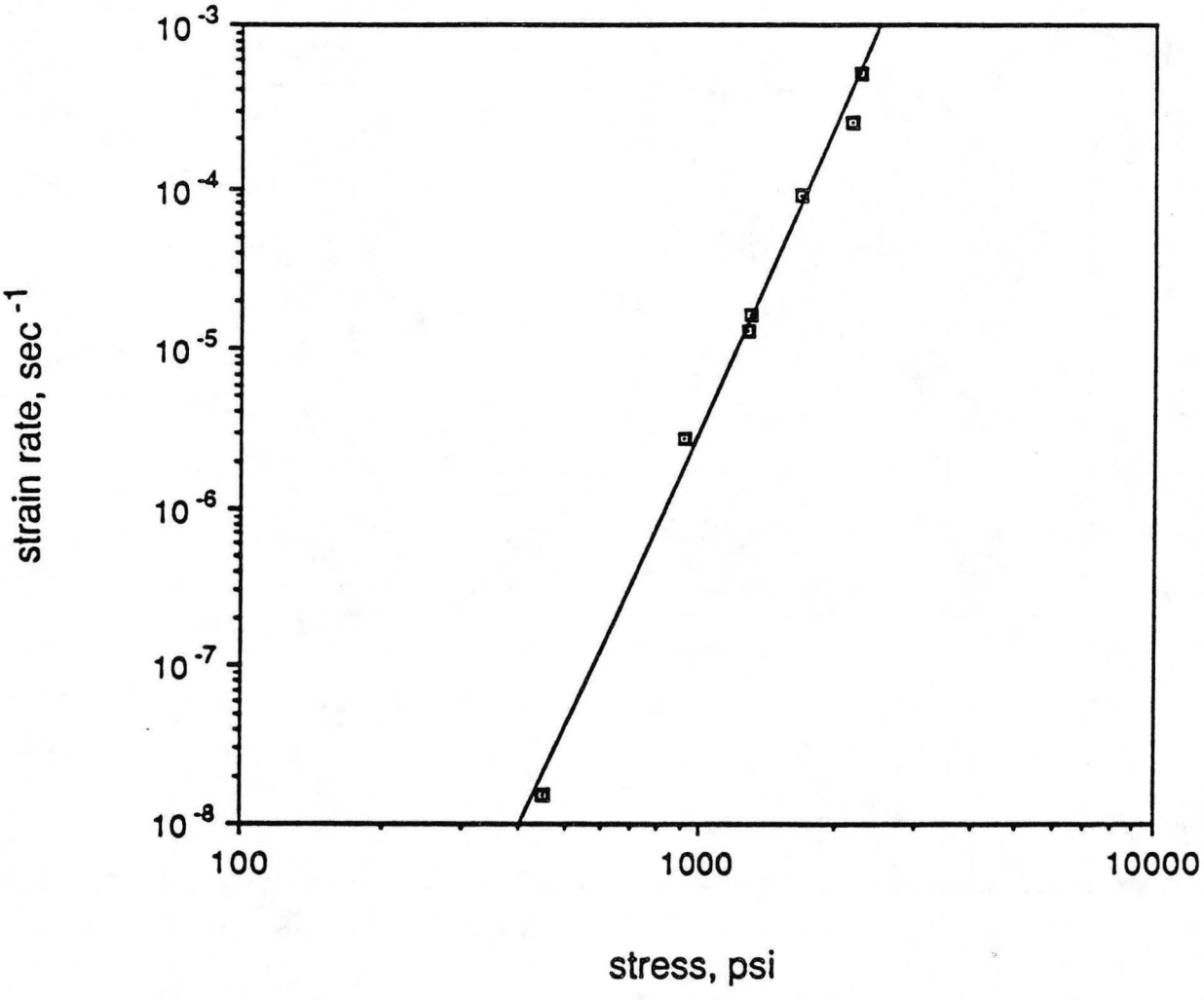

61.9Sn-38.1Pb, 75 C

Figure 3

STRAIN RATE vs 1/T

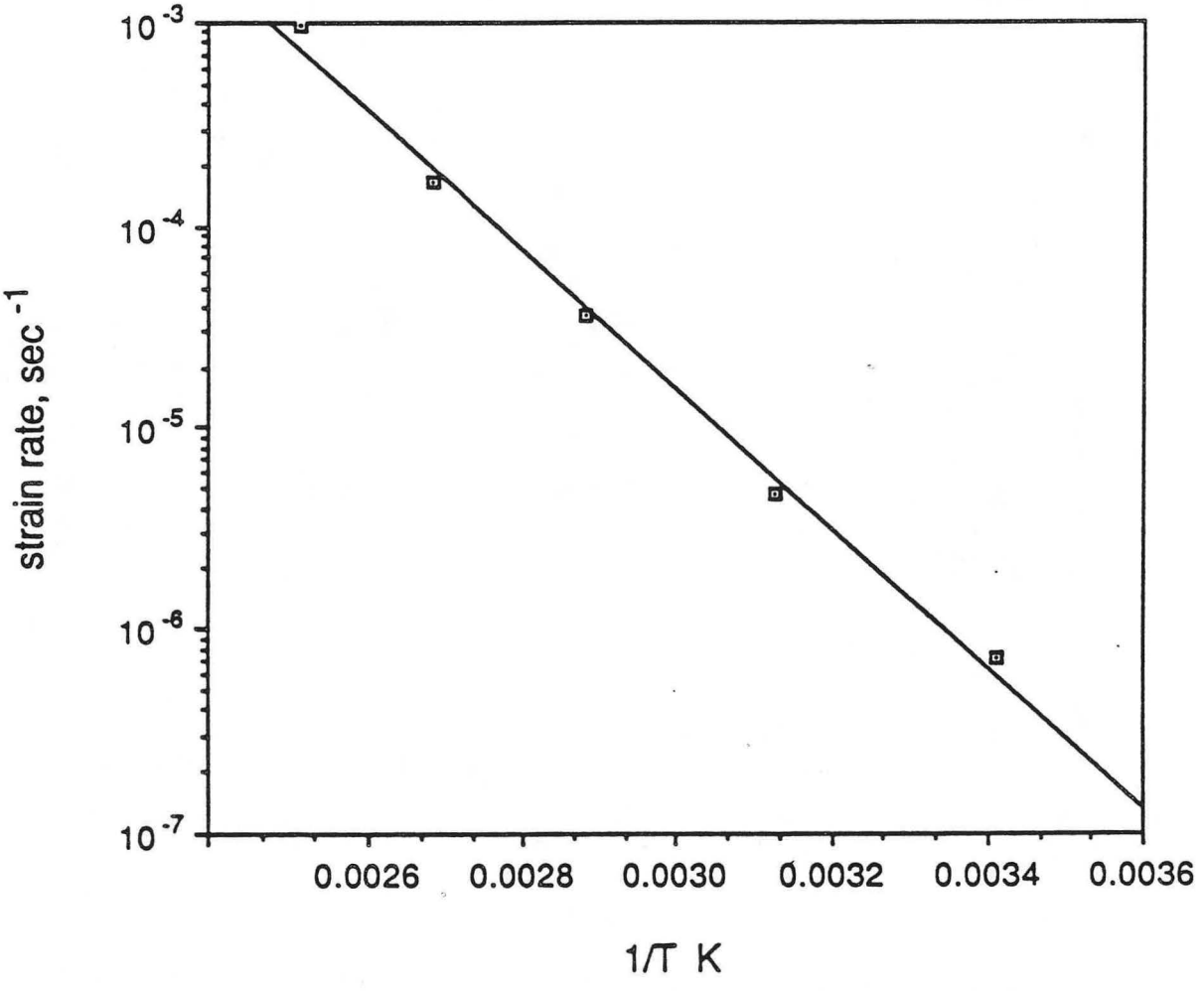

58Sn-48Pb-2Cd, 1280 psi

Figure 4

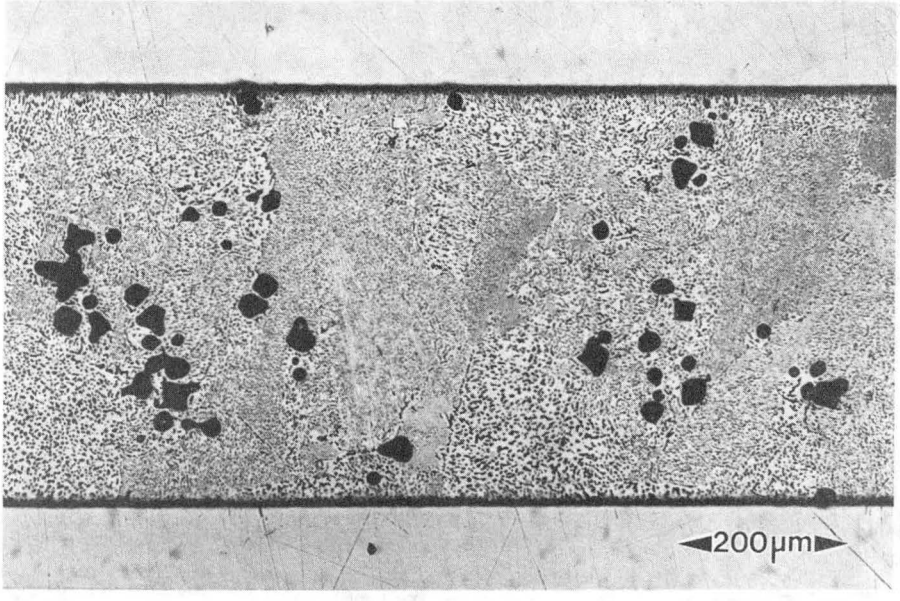

XBB 887 7081

Figure 5

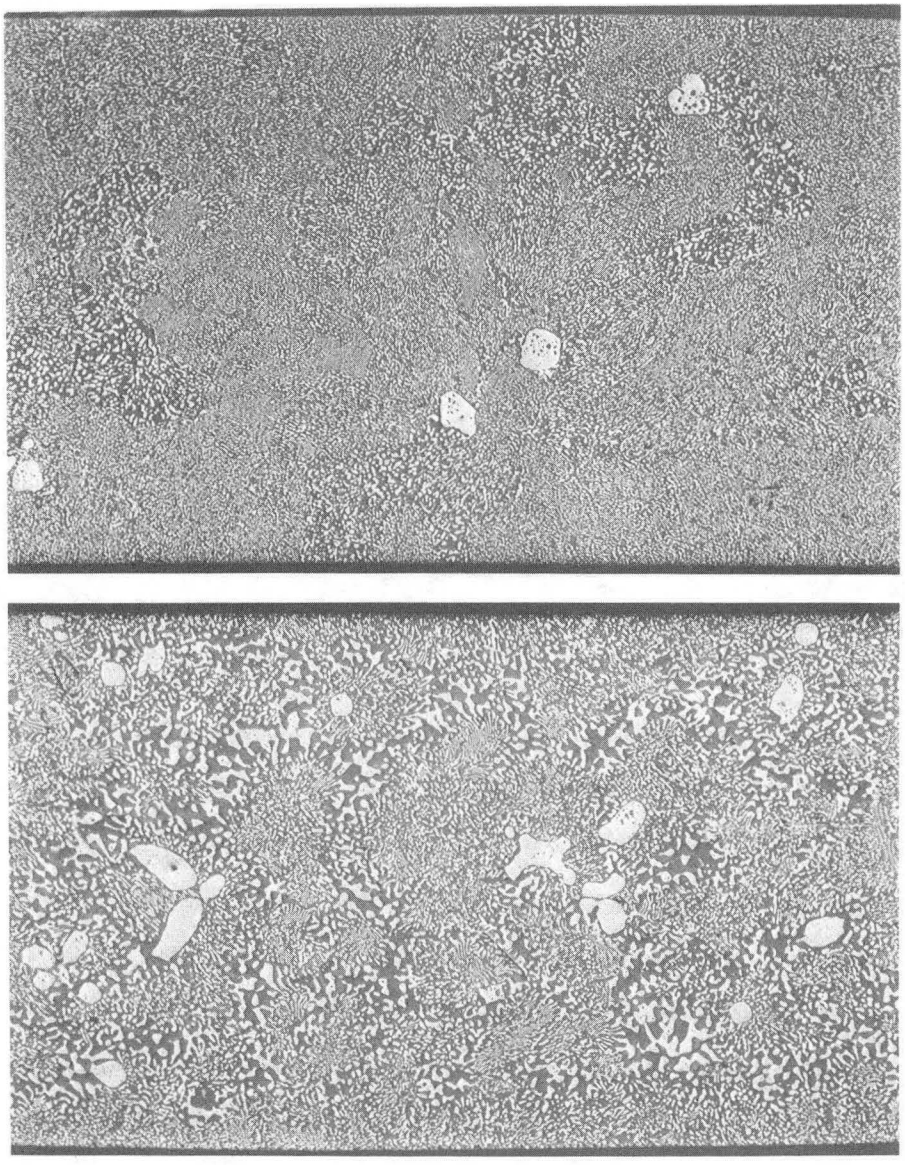

XBB 898 6549

Figure 6

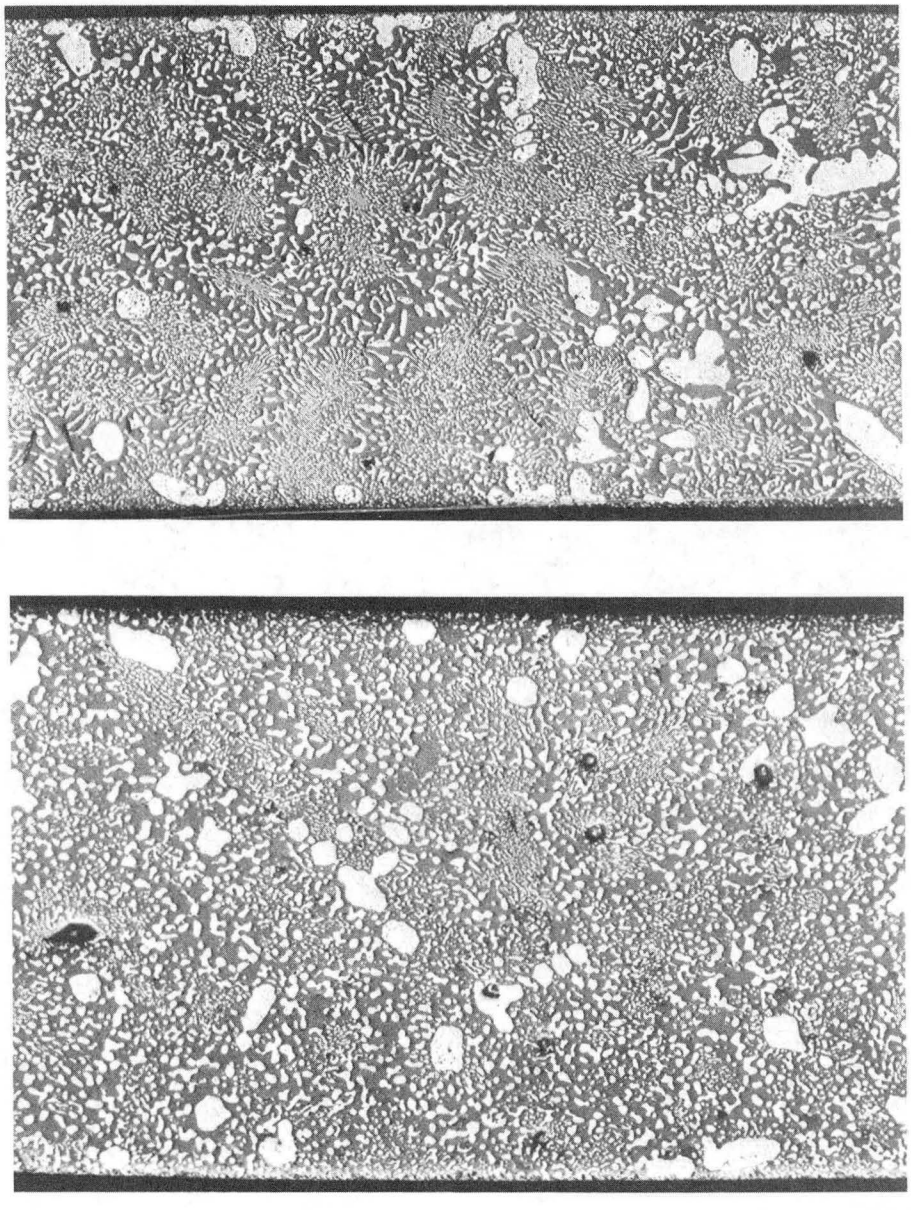

XBB 898 6542

Figure 7

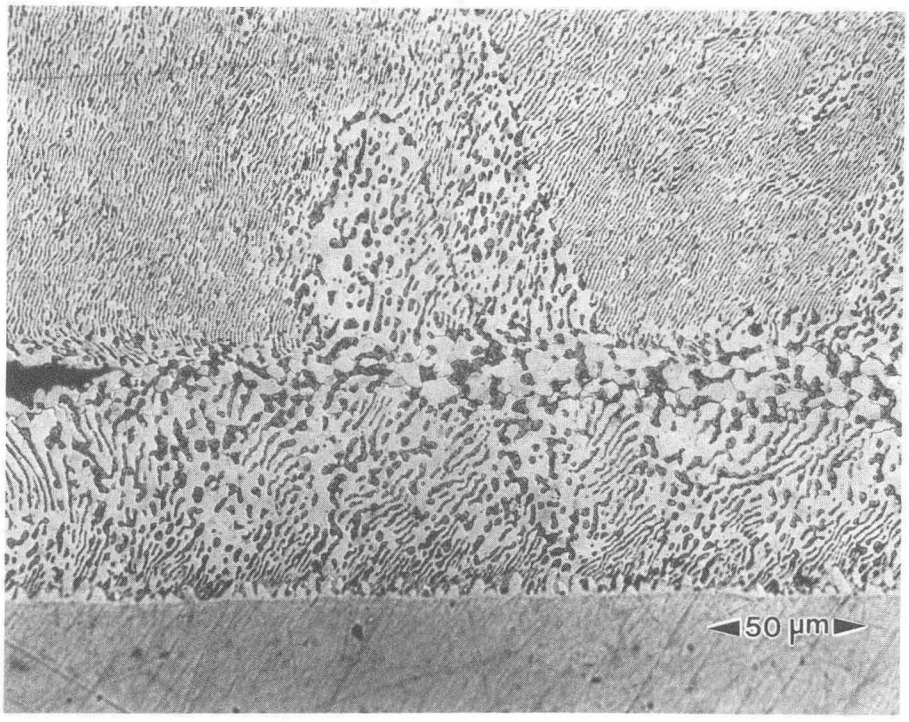

XBB 887-7083

Figure 8

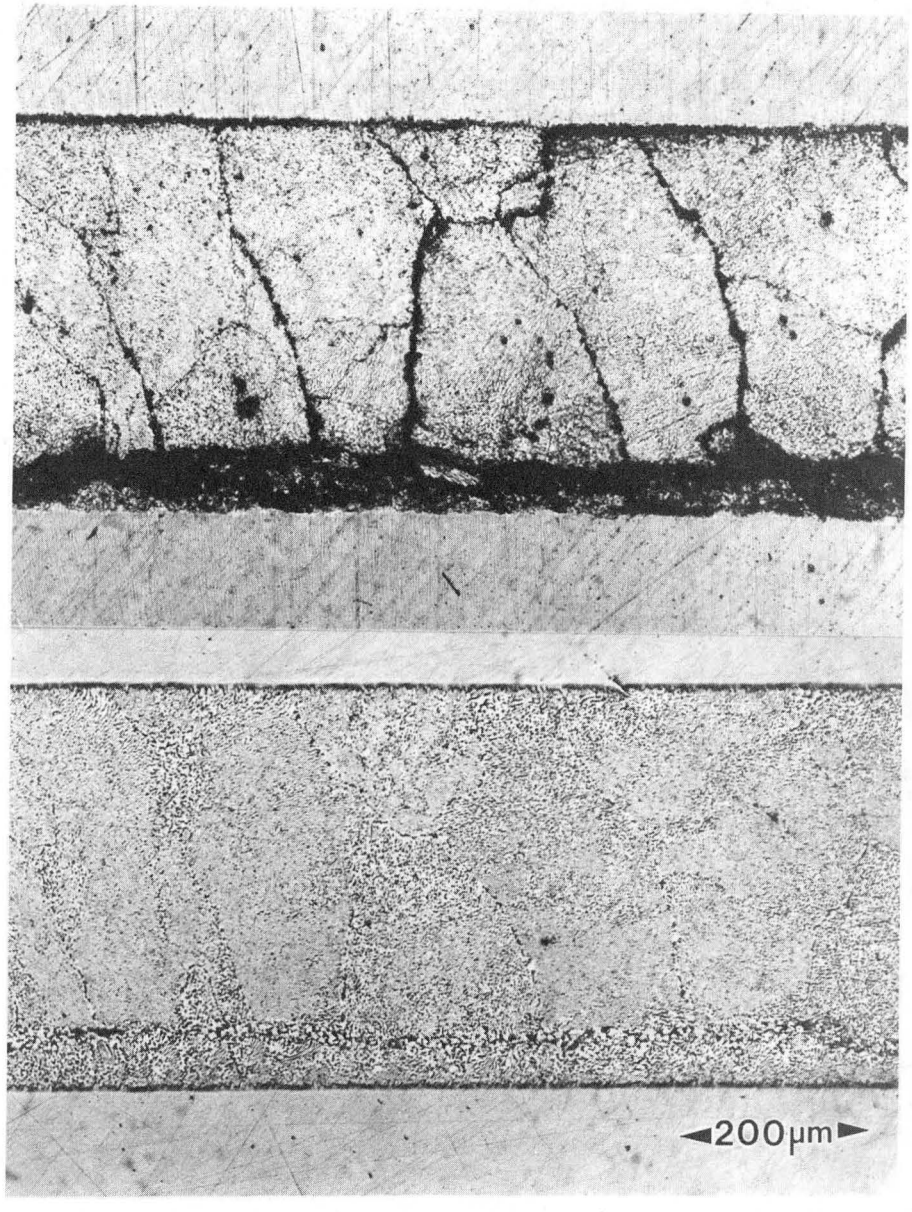

XBB 887 7084

Figure 9

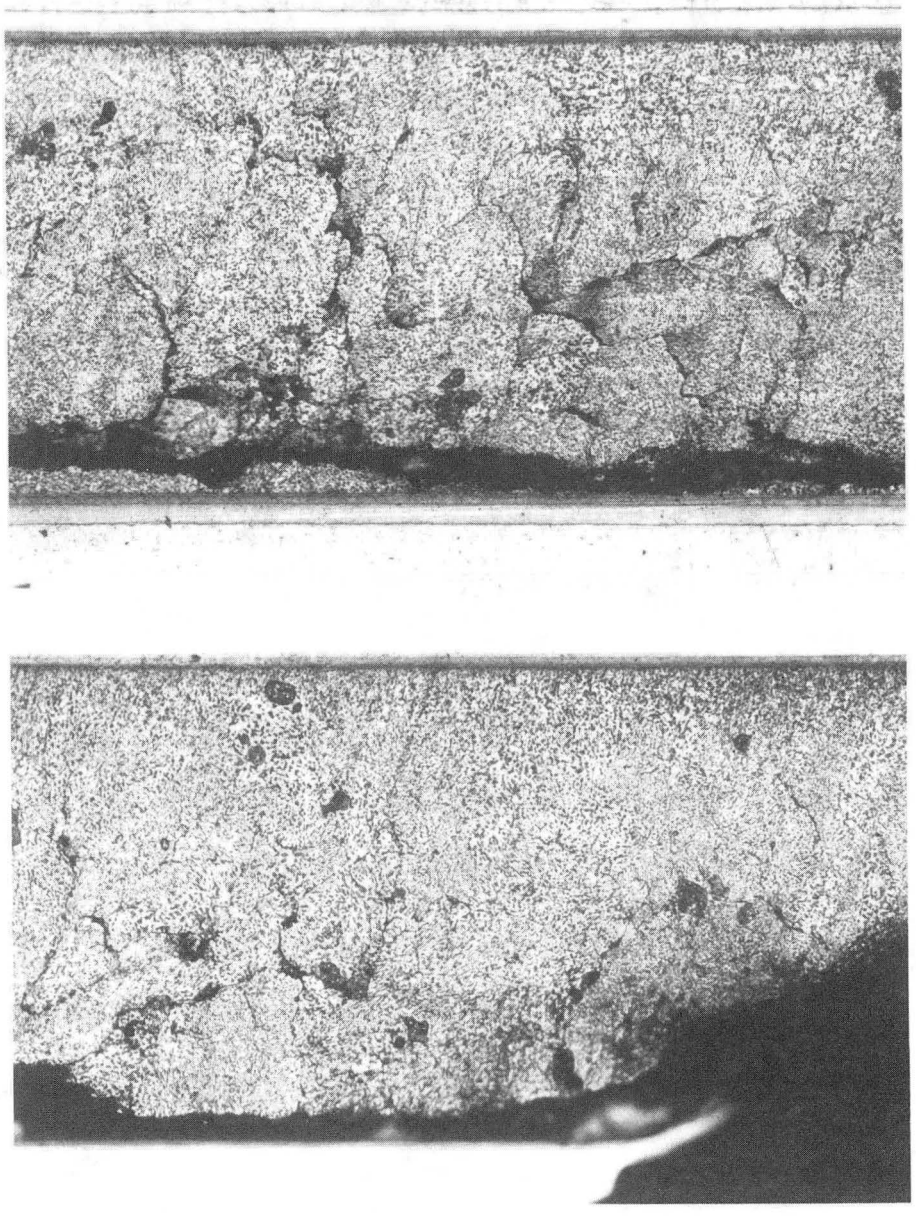

XBB 898 6553

Figure 10 (a)

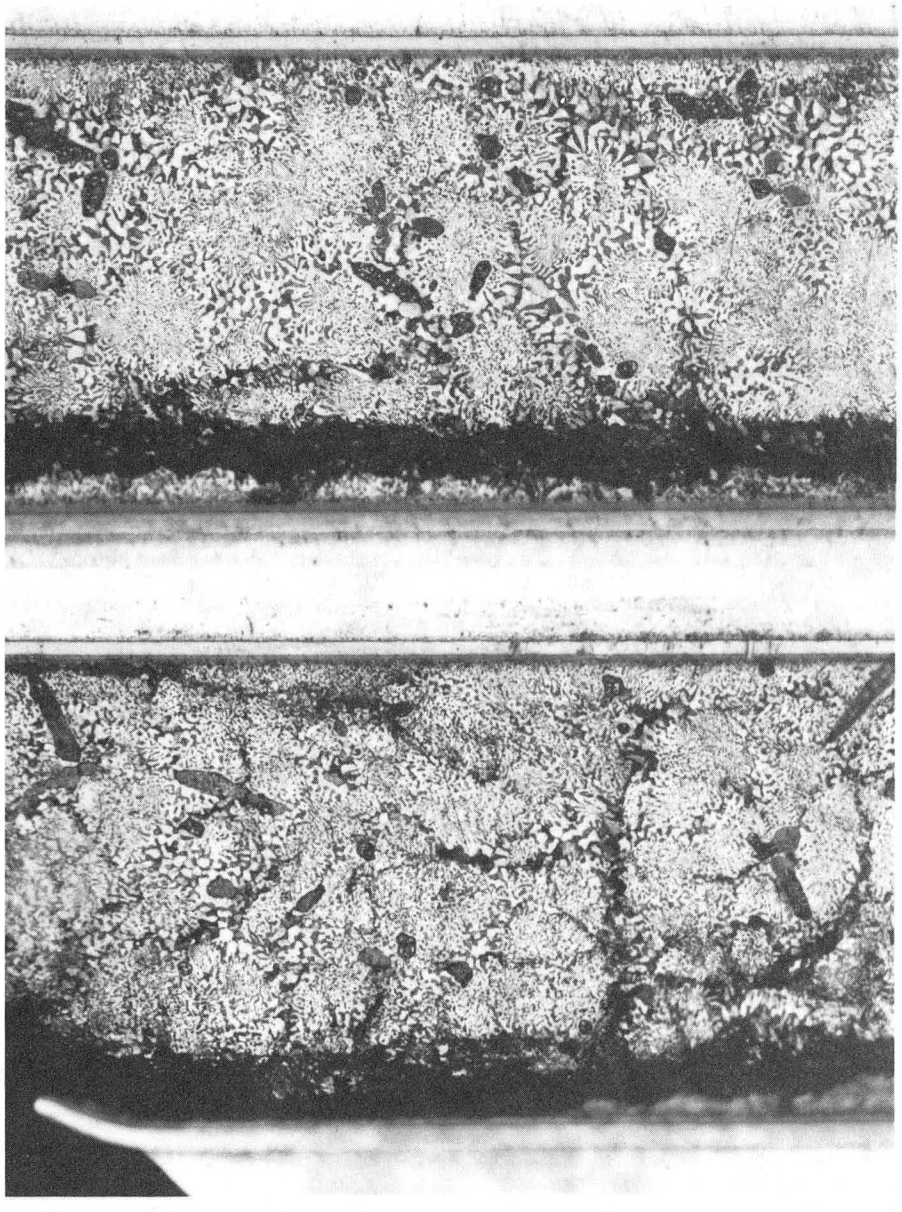

XBB 898 6555

Figure 10 (b)

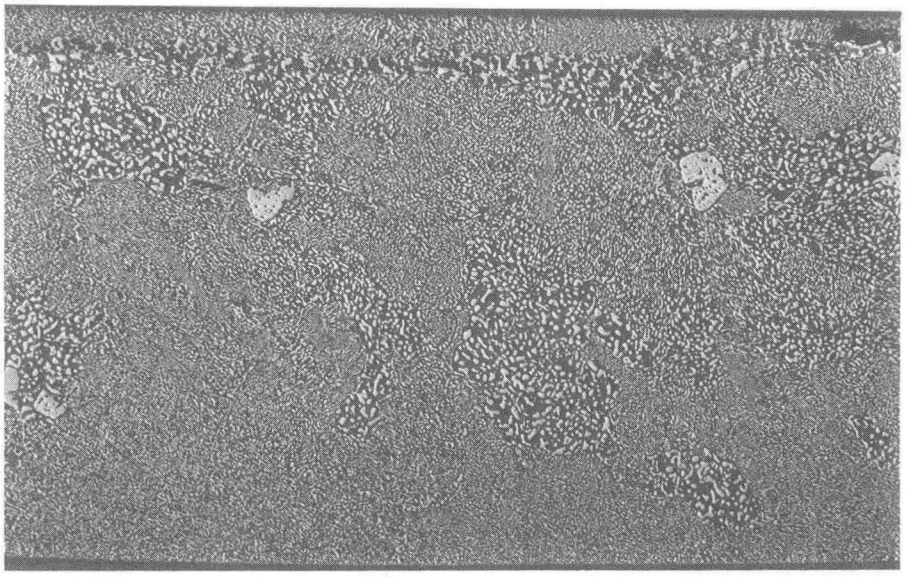

XBB 898 6556

Figure 11 (a)

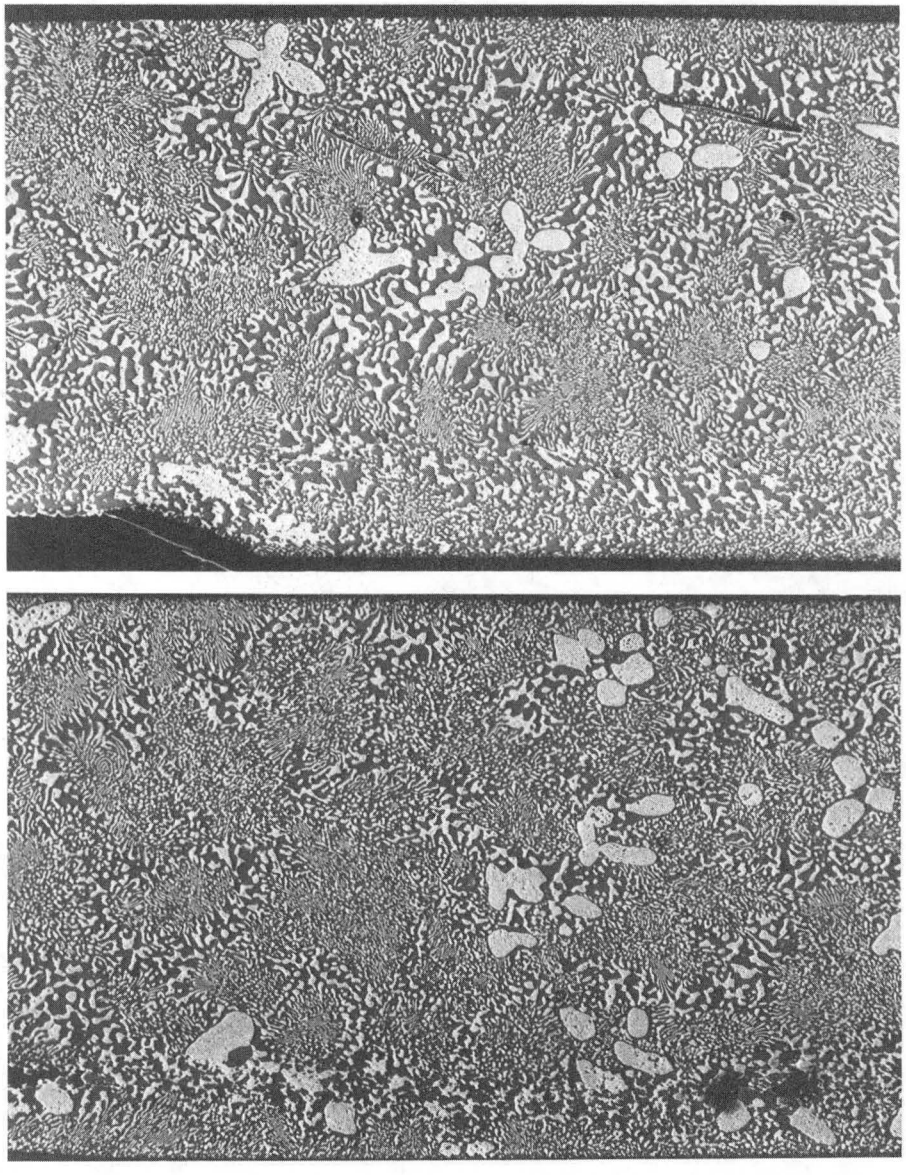

XBB 989 6552

Figure 11 (b)

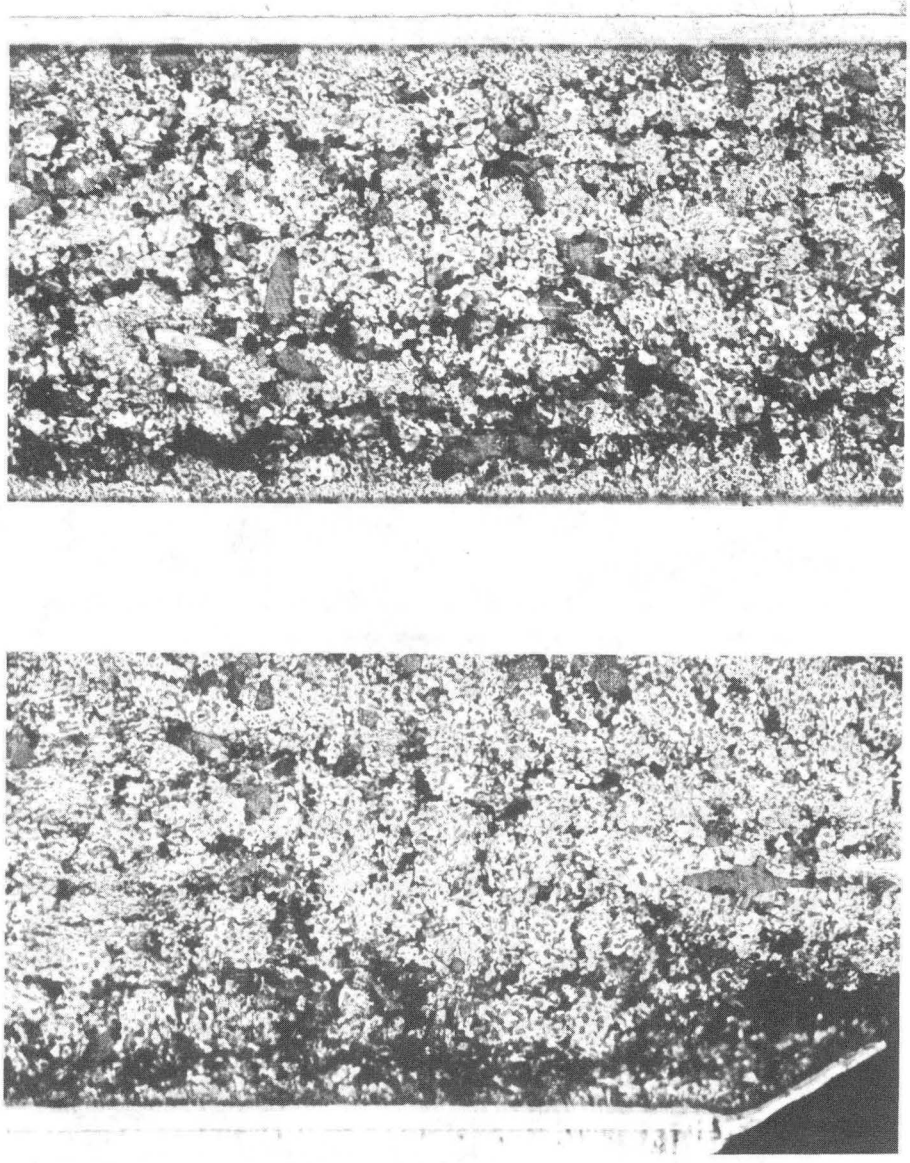

XBB 898 6541

Figure 12 (a)

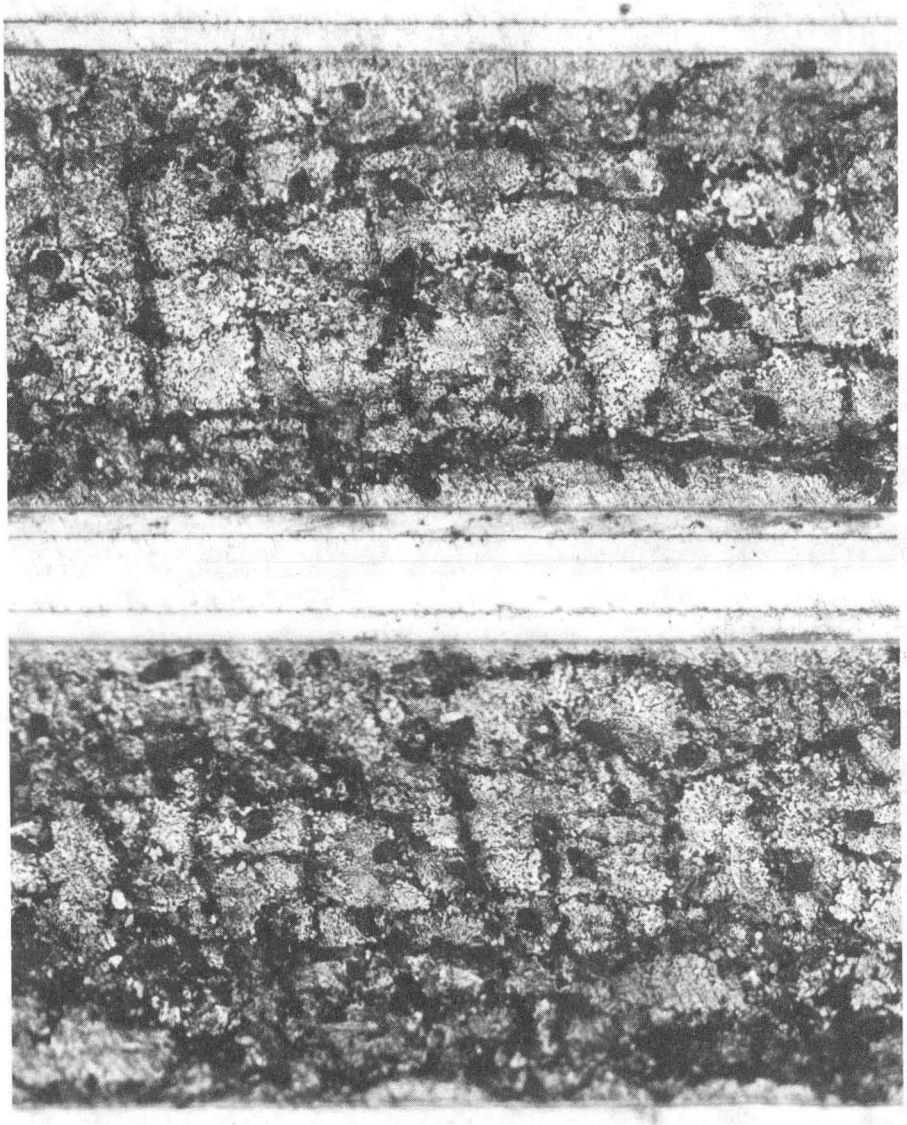

XBB 898 6550

Figure 12 (b)

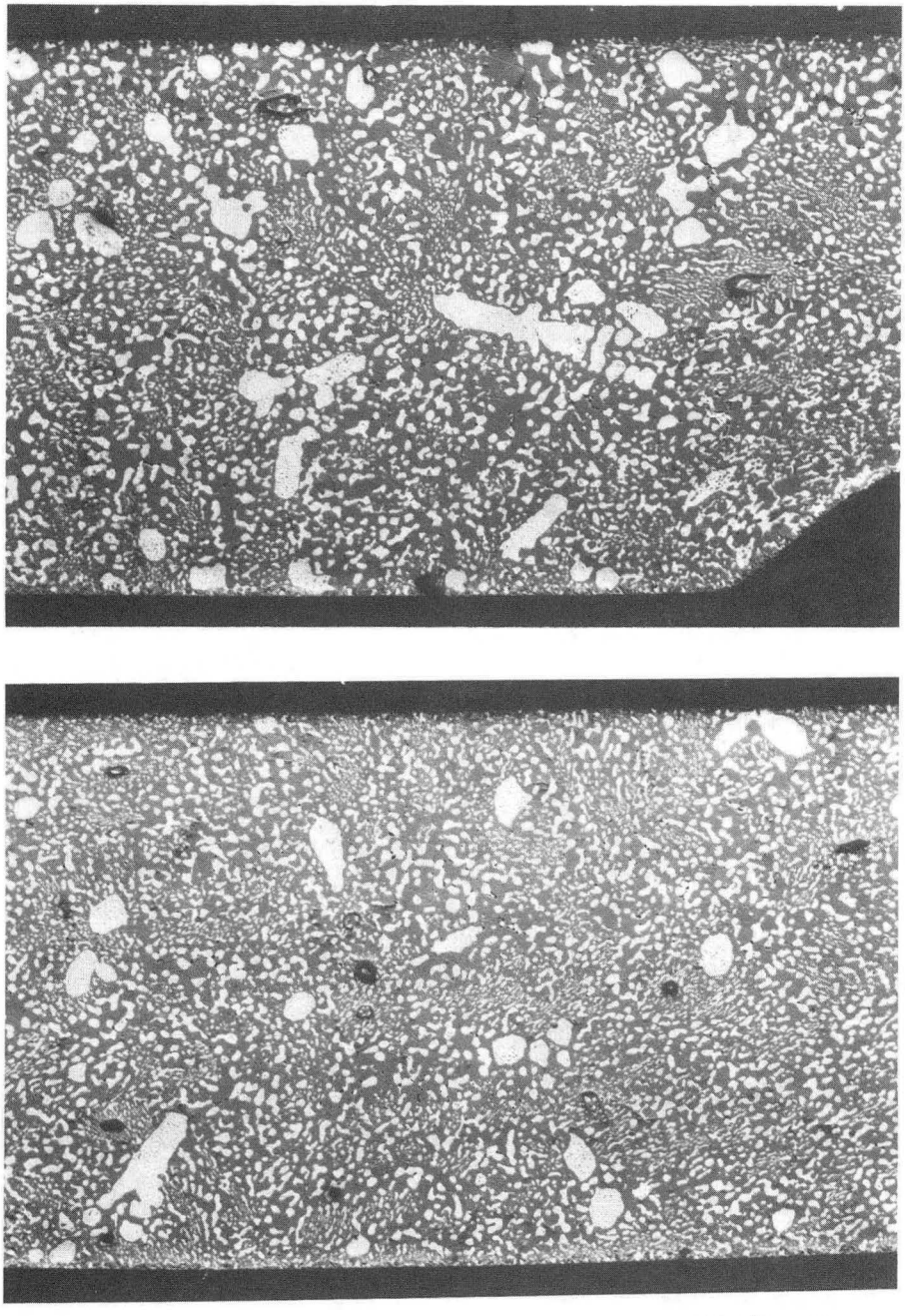

XBB 898 6551

Figure 13 (a)

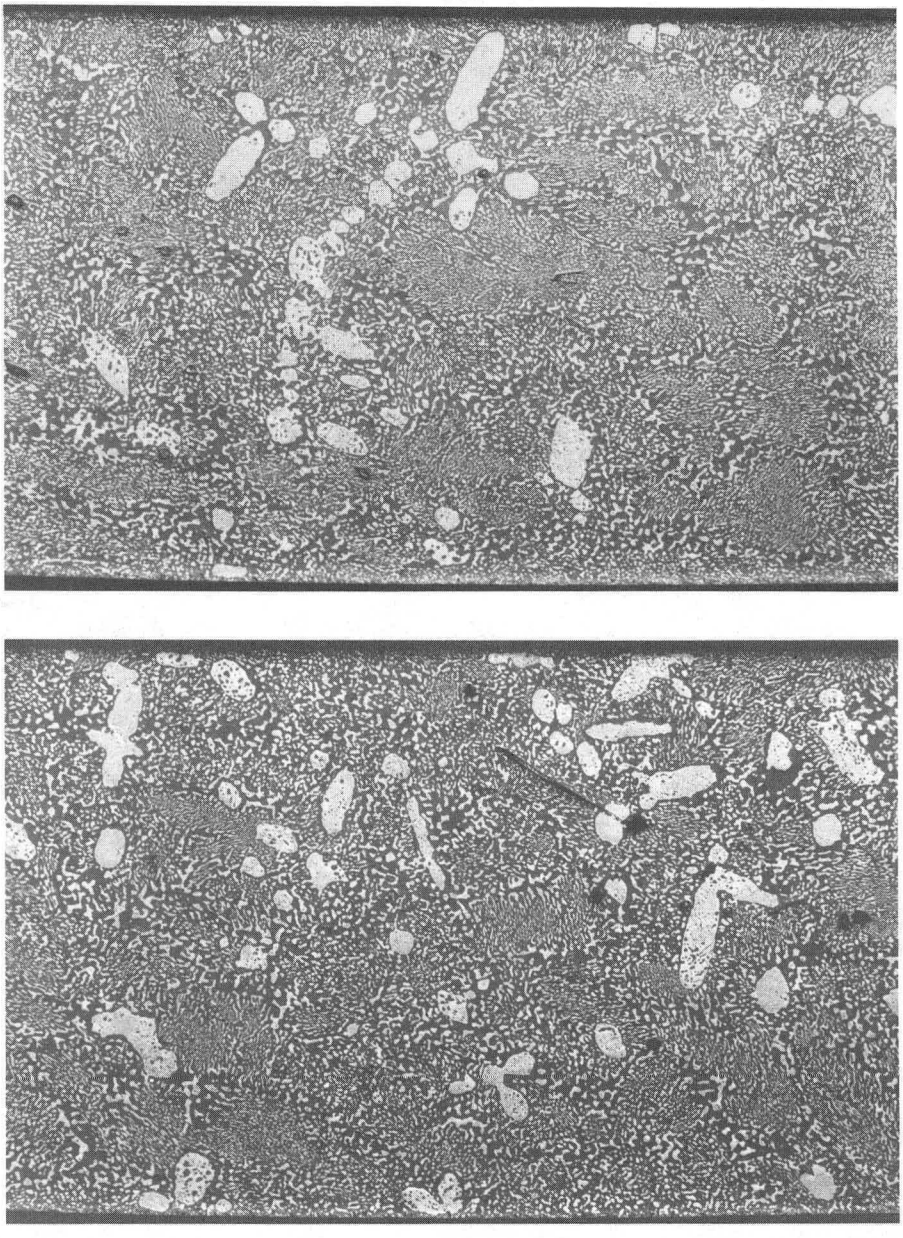

XBB 898 6554

Figure 13 (b)

LAWRENCE BERKELEY LABORATORY
CENTER FOR ADVANCED MATERIALS
1 CYCLOTRON ROAD
BERKELEY, CALIFORNIA 94720